Journal of Materials Chemistry C

RSC Publishing

PAPER

View Article Online
View Journal | View Issue

Cite this: *J. Mater. Chem. C*, 2013, **1**, 7513

High-performance electron-transporting hybrid rylenes with low threshold voltage†

Xiangguang Li,[ab] Chengyi Xiao,[ab] Wei Jiang*[a] and Zhaohui Wang*[a]

Received 20th August 2013
Accepted 23rd September 2013

DOI: 10.1039/c3tc31644k

www.rsc.org/MaterialsC

We present here a new family of hybrid rylene arrays (**3a–d**) by the combination of Stille coupling and C–H transformation *via* a facile one-pot synthesis. The π-expanded rylene diimides exhibit broadened and intensive optical absorption accompanied by higher electron affinity. The linear alkyl chain substituted NDI-diPDI-NDI (**3b**) revealed its electron transporting characteristics with good air stability and low threshold voltage.

Introduction

Rylene diimides as chromophores are attracting considerable attention in a variety of electronic devices owing to their good chemical and physical stabilities, high electron affinity, and easy chemical modification.[1] Naphthalene diimides (NDIs)[2] and perylene diimides (PDIs)[3] are perceived as the most important building blocks toward functional rylene dyes either by modification on imide or core positions. Especially, π-expanded rylenes are among the most promising representatives aiming at enhanced electron transport properties and ambient stability (Fig. 1).[4]

We have been focusing on the design and synthesis of lateral expansion of rylene diimides based on NDIs and PDIs with unique optoelectronic and supramolecular self-assembly behaviour.[5] Accordingly, a series of graphene-like triply-linked PDI arrays up to four units have been obtained by facile homocoupling of tetrahalogenated PDIs *via* Ullmann reaction and C–H transformation.[6] Especially, tetrachloro di(perylene diimides) (diPDIs) substituted by linear alkyl chains also demonstrated their good processibility and excellent electron mobilities as high as 4.65 $cm^2 V^{-1} s^{-1}$ *via* solution-processed single crystal transistors.[7] Furthermore, hybrid rylene arrays involving NDI and PDI moieties (NDI-PDI-NDI) have been prepared by a combination of Stille coupling and C–H transformation, and their use in organic thin-film transistors (OTFTs) has been explored as a consequence of excellent electron transport characteristics under ambient conditions.[8]

Inspired by these results, we assiduously pursued further expansion of rylene diimides along the equatorial axis by fusion of NDI and diPDI units to enrich the library of the π-expanded rylenes that will lead to more broadened absorption and electron affinity, thus providing more possibilities of facilitating electron transport and stabilization. Herein, hybrid rylene arrays (NDI-diPDI-NDI, **3**) have been obtained by a facile one-pot synthesis *via* a combination of Stille coupling and C–H transformation. As one of the biggest conjugated molecules, these new hybrid rylene dyes possess 18 six-membered carbon rings in the core and 8 imide groups at the edges. It was found that the π-expanded rylene diimides along the equatorial axis, **3**, not only broadened and enhanced optical absorptions, but also exhibited good thermal stability and high electron affinity. Employing them in thin-film transistors produced mobilities as

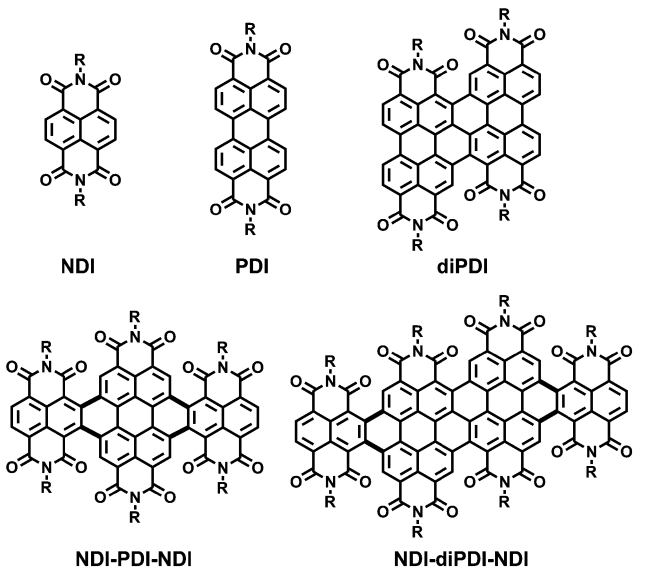

Fig. 1 Chemical structures of NDI, PDI, diPDI, and hybrid rylene arrays NDI-PDI-NDI and NDI-diPDI-NDI.

[a]*Beijing National Laboratory for Molecular Sciences, Key Laboratory of Organic Solids, Institute of Chemistry, Chinese Academy of Sciences, Beijing 100190, China. E-mail: jiangwei@iccas.ac.cn; wangzhaohui@iccas.ac.cn; Fax: +86-10-62653617; Tel: +86-10-62653617*

[b]*University of Chinese Academy of Sciences, Beijing, 100049, China. Fax: +86-10-62653617; Tel: +86-10-62653617*

† Electronic supplementary information (ESI) available: Thin-film absorptions, TGA, DSC, AFM, NMR, MS and representative transfer curves of **3a–d**. See DOI: 10.1039/c3tc31644k

high as 0.18 $cm^2 V^{-1} s^{-1}$ and an on/off current ratio up to 5.5×10^5 for linear alkyl chain substituted NDI-diPDI-NDI (**3b**) under ambient conditions.

Results and discussion

Design and synthesis

As illustrated in Scheme 1, hybrid rylene arrays (NDI-diPDI-NDI, **3a–d**) were synthesized by one-step of cross-coupling between tetrachloro-di(perylene diimides) (R-4CldiPDIs, **1**)[6a,7] and monostannyl naphthalene diimide (Sn-NDI, **2**),[8,9] which underwent Stille coupling and C–H transformation using $Pd(PPh_3)_4$ and CuI as the reagents in moderate yields of 20–40%. Four substituents were introduced into the backbone, since proper chain attachment would exert a remarkable influence on processability, molecular packing, and therefore charge transport characteristics.[10] The as-synthesized arrays are dark green solids and their structures are unambiguously characterized by mass spectrometry and NMR spectroscopy. They show good solubility in common organic solvents such as CH_2Cl_2, $CHCl_3$, THF, and chlorobenzene, which is a prerequisite for solution-processed electronic devices.

Optical, electrochemical and thermal properties

Room temperature absorption spectra of four hybrid rylene arrays **3a–d** were measured in $CHCl_3$ solution. As shown in Fig. 2a, the series exhibit broad absorption, which covers almost the whole spectrum of visible light. The spectra of compounds **3a–d** with various appending substituents on the imide positions are almost identical to each other with major bands at about 420, 560, 610, and 700 nm, implying that the substituents have little effect on optical properties as expected. It was observed that the absorption maxima of **3a–d** are bathochromically shifted to about 10–18 nm with respect to that of the parent diPDI (λ_{max} = 684 nm).[11] The further bathochromic shift is indicative that the expansion of the π-system along the equatorial axis can lead to effective communication between NDI and diPDI and correspondingly large delocalization of electronic wave functions.[12] The optical band gaps of about 1.68 eV were determined from the onset absorption wavelengths of these compounds (~736 nm). The results suggest that the fusion of NDI and diPDI units narrows the HOMO–LUMO gap, comparing the parent diPDI[11] and the reported NDI-PDI-NDI.[8] Their thin-film absorptions (Fig. S1†) were more or less red-shifted and broadened compared to those in solutions, suggesting that a certain degree of aggregation is present in solution at room temperature.

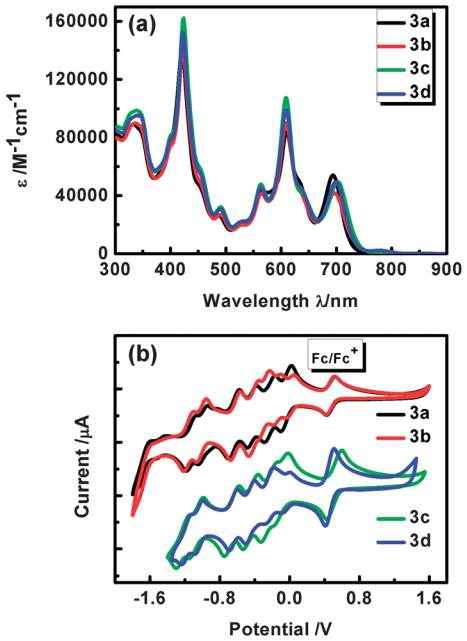

Fig. 2 (a) UV-vis absorption spectra of hybrid arrays **3a–d** in $CHCl_3$ solution (1×10^{-5} mol L^{-1}). (b) Cyclic voltammograms of hybrid arrays **3a–d** in CH_2Cl_2, scan rate = 100 mV s^{-1} (electrolyte: 0.1 M n-Bu_4NPF_6).

Cyclic voltammograms (CV) of **3a–d** in CH_2Cl_2 were measured to investigate their electrochemical properties (Fig. 2b). Eight reduction waves were detected for **3a** and **3b**, and six reduction waves for **3c** and **3d**, while no oxidation wave could be observed within the solvent/electrolyte window. The half-wave reduction potentials *vs.* Fc/Fc^+, as well as the LUMO levels estimated from the onset of reduction potentials are listed in Table 1. The LUMO levels of compounds **3a–d** are almost below

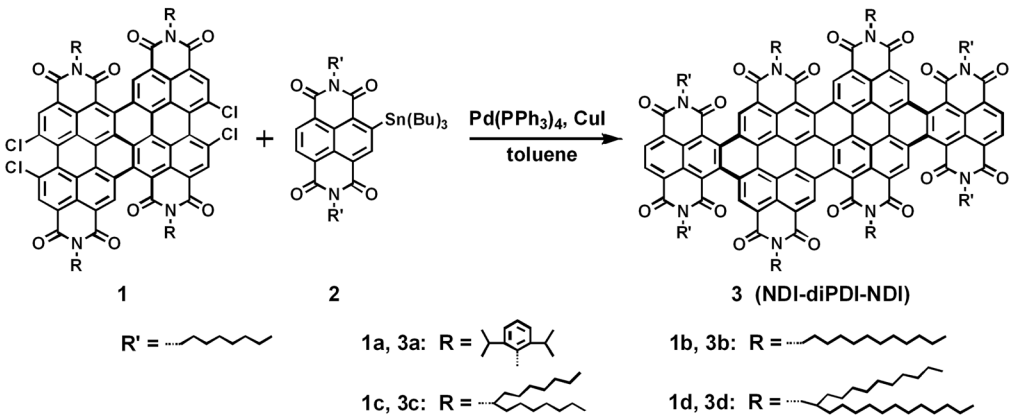

Scheme 1 Synthetic route to hybrid rylene diimide arrays.

Table 1 Optical, electrochemical and thermal properties of hybrid rylene arrays **3a–d**

Compounds	λ_{max}^{sol} [a] [nm]	ε [a] [M^{-1} cm^{-1}]	λ_{max}^{film} [b] [nm]	E_{1r} [c] [V]	E_{2r} [c] [V]	E_{3r} [c] [V]	E_{4r} [c] [V]	E_{5r} [c] [V]	E_{6r} [c] [V]	E_{7r} [c] [V]	E_{8r} [c] [V]	E_{LUMO} [d] [eV]	E_g [e] [eV]	T_{deg} [f] [°C]
3a	694	54 037	696	−0.51	−0.70	−0.90	−1.11	−1.47	−1.60	−1.95	−2.14	−4.35	1.70	419
3b	697	41 657	727	−0.51	−0.61	−0.75	−0.88	−1.09	−1.48	−1.63	−2.12	−4.40	1.68	415
3c	702	49 580	713	−0.60	−0.75	−0.96	−1.17	−1.58	−1.74	—	—	−4.27	1.68	394
3d	699	49 389	717	−0.49	−0.69	−0.91	−1.10	−1.50	−1.64	—	—	−4.37	1.68	416

[a] Measured in dilute $CHCl_3$ solution (1.0×10^{-5} M). [b] Measured in the films on quartz substrates (as-spun). [c] Half-wave potentials in CH_2Cl_2 solution *vs.* Fc/Fc^+, performed in *n*-Bu_4NPF_6/CH_2Cl_2 (0.1 M), scan rate 100 mV s^{-1}. [d] LUMO estimated by the onset of reduction peaks and calculated according to $E_{LUMO} = -(4.8 + E_{onset})$. [e] Calculated by the onset of absorption in $CHCl_3$ solution according to $E_g = 1240/\lambda_{onset}$. [f] Decomposition temperature determined by TGA corresponding to 5% weight loss at 10 °C min^{-1} under nitrogen flow.

−4.3 eV, indicating the high electron affinity to facilitate electron injection, and therefore, potentially low threshold voltage and good air stability for *n*-channel OFETs.[13]

Thermal stability of compounds **3a–d** was evaluated by thermogravimetric analysis (TGA) and differential scanning calorimetry (DSC). The TGA measurements revealed that all of the compounds are thermally stable over 390 °C with a 5% weight loss under nitrogen (Fig. S2†). The DSC curves of compounds **3a** and **3b** showed no phase transition phenomenon on heating and cooling processes from −80 °C to 350 °C before their decomposition. While the melting points of **3c** and **3d** from DSC measurements were 287 °C and 235 °C, respectively (Fig. S3†), the TGA and DSC results revealed that they exhibited impressive thermal stability.

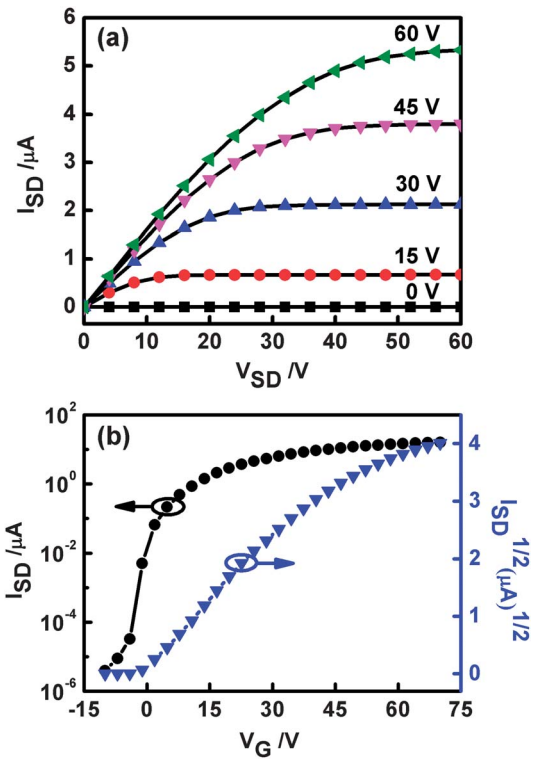

Fig. 3 Representative output (a) and transfer (b) characteristics of OTFTs of hybrid array **3b** after annealing at 200 °C, $V_{sd} = 70$ V.

OTFT characteristics

A bottom-gate top-contact device configuration afforded investigation of the transporting properties of compounds **3a–d**. Films of the semiconductors with a thickness of 40–60 nm were spin coated from their chloroform–*n*-hexane solutions (10 mg ml^{-1}, 3000 r min^{-1}) onto octadecyltrichlorosilane (OTS)-modified SiO_2/Si (300 nm) substrates. The gold (Au) source–drain electrodes with width/length of 240 μm/30 μm were deposited on the semiconductor films through a shadow mask. All devices were operated under an ambient atmosphere. Representative transfer and output characteristics of OTFTs based on **3b** are given in Fig. 3.

Table 2 summarized the optimized performances of thin-film transistors for **3a–d** after thermal annealing. As expected from the low-lying LUMO levels (∼−4.3 eV), the OTFTs fabricated from **3a–d** showed good *n*-channel characteristics under ambient conditions, in which **3a** bearing bulky substituents showed the electron mobilities in the magnitude of 10^{-3} cm^2 V^{-1} s^{-1}, while devices based on **3c** and **3d** with branched alkyl chain substituents exhibited moderate electron mobilities of 0.054 and 0.074 cm^2 V^{-1} s^{-1}, respectively. In particular, linear alkyl chain substituted NDI-diPDI-NDI **3b** expressed the highest electron mobility up to 0.18 cm^2 V^{-1} s^{-1} with an on/off current ratio up to 5.5×10^5 after annealing at 240 °C. It should be noted that **3b** with linear alkyl chains showed one order of magnitude electron mobility higher than **3c** and **3d** with branched alkyl chains (10^{-1} *vs.* 10^{-2} cm^2 V^{-1} s^{-1}). The results demonstrated that the alkyl side chains play an important role in crystallinity, molecular packing, and therefore OTFT performances. As observed in

Table 2 Device performance of thin-film transistors for compounds **3a–d** at optimized annealing temperature in air

Compounds	T [a] [°C]	μ_e [b] [cm^2 V^{-1} s^{-1}]	V_T [c] [V]	I_{on}/I_{off} [d]
3a	200	0.003	0.35	6.5×10^4
3b	240	0.18	0.95	5.5×10^5
3c	240	0.054	9.91	3.5×10^6
3d	200	0.074	11.6	6.1×10^6

[a] Optimized annealing temperature. [b] Electron mobility. [c] Threshold voltage. [d] On/off current ratio.

Table 2, all devices exhibited relatively low threshold voltage. It was observed that the threshold voltage values of **3c** and **3d** were largely higher than those of **3a** and **3b**, the possible reason for this could be attributed to their difference in molecular packing, which is caused by the alkyl side chains and therefore exerted great influence on OTFT performances, or the existence of defects in the thin films of the latter two compounds.[14] In addition, the long-term air stability was monitored by measuring the OTFT performance as a function of time for the higher mobility compound **3b** (Fig. S5†), the devices showed excellent air stability without obvious decrease in mobility and on/off ratio for 100 days.

Conclusions

In conclusion, a novel family of hybrid rylene arrays (NDI-diPDI-NDI) has been presented by a facile one-pot synthesis *via* the combination of Stille coupling and C–H transformation. Further expansion of rylene diimides along the equatorial axis using diPDI fusing with NDI units elaborated a broadened and intensive optical absorption accompanied by higher electron affinity. The best OTFT performance has been achieved by the linear alkyl chain substituted one which showed an electron mobility as high as 0.18 $cm^2 V^{-1} s^{-1}$ with an on/off current ratio up to 5.5×10^5 under ambient conditions. Excellent device stability in air and quite low threshold voltage make these kinds of materials promising in practical applications. Further research on the processing engineering including the device structure and technology are currently underway.

Experimental

Materials and general methods

All chemicals were purchased from commercial suppliers and used without further purification unless otherwise specified. The solvent DMSO from Alfa Aesar was dry and used directly, and toluene was distilled over sodium and benzophenone. ^{1}H NMR and ^{13}C NMR spectra were recorded in deuterated solvents using a Bruker DMX 300 (300 MHz), or a Bruker ADVANCE 400 (400 MHz), or a Bruker ADVANCE 600 (600 MHz) NMR Spectrometer. NMR chemical shifts are reported in ppm using the residual protonated solvent as an internal standard. Mass spectra (MALDI-TOF-MS) were determined using a Bruker BIFLEX III Mass Spectrometer.

Absorption spectra were measured with a Hitachi (model U-3010) UV-Vis spectrophotometer in a 1 cm quartz cell. Cyclic voltammograms (CVs) were recorded using a Zahner IM6e electrochemical workstation at a scan rate of 100 mV s^{-1}, using glassy carbon discs as the working electrodes, Pt wire as the counter electrode, Ag/AgCl electrode as the reference electrode. 0.1 M tetrabutylammonium hexafluorophosphate (Bu_4NPF_6) dissolved in CH_2Cl_2 (HPLC grade) was employed as the supporting electrolyte, which was calibrated by the ferrocene/ferrocenium (Fc/Fc^+) as the redox couple. CH_2Cl_2 was freshly distilled prior to use. Thermogravimetric analysis (TGA) measurements were performed using a Shimadzu DTG 60 instrument at a heating rate of 10 °C min^{-1} under a N_2 atmosphere from room temperature to 550 °C and the reported decomposition temperatures represent the temperatures observed at 5% mass loss. Differential scanning calorimetry (DSC) analyses were recorded using a TA DSC 2010 instrument under a dry nitrogen flow, heating from −80 °C to 350 °C and cooling from 350 °C to −80 °C at a rate of 10 °C min^{-1}.

The OFET characteristics were measured in air at room temperature using a Keithley 4200 SCS semiconductor parameter analyzer. The mobilites were calculated from the saturation region with the following equation: $I_{SD} = (W/2L)C_i\mu(V_G - V_T)^2$, where I_{SD} is the drain–source current, W is the channel width, L is the channel length, μ is the field-effect mobility, C_i is the capacitance per unit area of the gate dielectric layer, and V_G and V_T are the gate voltage and threshold voltage, respectively.

Tetrachloro-di(perylene diimides) (R-4CldiPDIs, **1**)[6a,7] and monostannyl naphthalene diimide (Sn-NDI, **2**)[8] were synthesized and purified according to our previous work.

General synthetic procedure for hybrid rylene diimide arrays 3a–d

A mixture of Sn-NDI (**2**, 1.1 mmol) and different substituted R-4CldiPDIs (**1**, 0.5 mmol), in the presence of $Pd(PPh_3)_4$ (58 mg, 0.05 mmol) and CuI (10 mg, 0.052 mmol) reflux in dry toluene (30 ml) under argon for 12 h, after cooling to room temperature, the solvent was concentrated *via* rotary evaporation. The crude product was purified by silica gel chromatography (petroleum ether to dichloromethane), followed by recrystallization from dichloromethane–methanol to yield dark green solids.

Compound 3a. Yield: 22%. ^{1}H NMR (400 MHz, $CDCl_3$, 298 K) δ = 10.64 (s, 2H), 10.49 (s, 2H), 10.29 (s, 2H), 9.09 (s, 4H), 7.48–7.58 (m, 4H), 7.39–7.41 (m, 8H), 4.27 (m, 8H), 2.91 (m, 8H), 1.89–1.91 (m, 8H), 1.22–1.44 (m, 88H), 0.83–0.86 (m, 12H). ^{13}C NMR (150 MHz, $CDCl_3$, 298 K) δ = 164.63, 164.58, 164.55, 163.92, 163.87, 163.45, 162.56, 137.26, 137.11, 135.85, 134.89, 134.39, 133.14, 132.70, 131.37, 131.26, 130.08, 130.00, 129.24, 128.79, 128.33, 127.95, 127.84, 127.52, 127.39, 127.35, 127.32, 127.25, 126.79, 126.72, 125.88, 124.42, 124.39, 123.41, 122.72, 122.50, 122.43, 121.69, 121.43, 121.31, 120.70, 119.98, 42.53, 32.11, 29.64, 29.58, 29.56, 29.45, 29.43, 28.37, 28.33, 27.60, 27.57, 24.79, 24.41, 24.16, 22.93, 14.45. MS (MALDI-TOF): calcd for M, 2388.1; found, 2388.1.

Compound 3b. Yield: 26%. ^{1}H NMR (300 MHz, 1,1,2,2-tetrachloroethane-d_2, 375 K) δ = 10.44 (s, 2H), 10.14 (s, 2H), 9.79 (s, 2H), 9.03 (s, 2H), 8.91 (s, 2H), 4.64 (m, 4H), 4.48 (m, 4H), 4.29 (m, 4H), 4.05 (m, 4H), 2.13 (m, 16H), 1.35–1.65 (m, 112H), 0.87–1.00 (m, 24H). ^{13}C NMR (75 MHz, 1,1,2,2-tetrachloroethane-d_2, 375 K) δ = 163.90, 162.24, 162.14, 162.03, 161.87, 160.96, 160.20, 134.96, 133.06, 133.01, 132.80, 132.07, 131.67, 131.04, 128.24, 126.07, 125.95, 125.49, 125.29, 125.04, 124.83, 124.61, 124.50, 124.10, 124.02, 123.75, 122.78, 121.76, 120.75, 119.88, 119.55, 119.37, 119.04, 118.58, 118.21, 41.50, 40.94, 40.49, 40.35, 30.85, 30.76, 30.41, 28.74, 28.64, 28.53, 28.24, 28.12, 27.81, 27.67, 27.45, 27.26, 27.10, 26.60, 26.53, 26.32, 21.45, 12.88, 12.75. MS (MALDI-TOF): calcd for M^-, 2420.3; found, 2420.3.

Compound 3c. Yield: 40%. ^{1}H NMR (400 MHz, $CDCl_3$, 298 K) δ = 10.60 (s, 2H), 10.43 (s, 2H), 10.24 (s, 2H), 9.12 (s, 4H), 5.56

(m, 2H), 5.39 (m, 2H), 4.40–4.41 (m, 8H), 2.41 (m, 8H), 2.04 (m, 16H), 1.26–1.58 (m, 120H), 0.83–0.91 (m, 36H). ^{13}C NMR (150 MHz, $CDCl_3$, 298 K) δ = 165.88, 165.28, 165.23, 164.86, 164.02, 163.78, 163.68, 162.73, 136.95, 136.38, 135.72, 135.20, 134.98, 134.81, 133.00, 131.67, 131.25, 128.48, 128.29, 127.72, 127.46, 127.30, 127.21, 126.99, 126.57, 126.36, 125.51, 123.57, 122.62, 122.35, 122.29, 122.03, 121.38, 120.80, 120.65, 119.34, 118.36, 55.66, 55.41, 42.47, 42.41, 32.93, 32.33, 32.28, 32.23, 30.05, 30.01, 29.82, 29.68, 28.65, 27.75, 27.57, 23.07, 23.05, 23.01, 14.49, 14.42. MS (MALDI-TOF): calcd for M^-, 2588.5; found, 2588.8.

Compound 3d. Yield: 25%. ^{1}H NMR (400 MHz, $CDCl_3$, 298 K) δ = 10.61 (s, 2H), 10.44 (s, 2H), 10.26 (s, 2H), 9.13 (s, 4H), 4.50 (m, 4H), 4.38 (m, 12H), 2.65 (m, 2H), 2.17 (m, 2H), 1.99 (m, 8H), 1.17–1.32 (m, 200H), 0.88–0.89 (m, 12H), 0.79–0.81 (m, 24H). ^{13}C NMR (150 MHz, $CDCl_3$, 298 K) δ = 165.91, 164.47, 163.96, 163.47, 162.67, 162.55, 136.68, 135.48, 135.20, 134.80, 133.11, 128.44, 128.17, 127.76, 127.54, 127.34, 127.09, 126.70, 126.56, 126.42, 126.39, 125.65, 125.47, 125.43, 125.18, 125.01, 123.56, 122.81, 122.61, 122.30, 121.99, 121.46, 121.14, 120.98, 120.70, 120.41, 119.94, 119.65, 42.51, 37.60, 37.22, 32.72, 32.41, 32.23, 30.70, 30.62, 30.18, 30.11, 29.84, 29.72, 29.67, 28.62, 28.34, 27.69, 27.47, 27.04, 26.77, 23.18, 23.06, 22.99, 14.48, 14.41. MS (MALDI-TOF): calcd for M^-, 3094.1; found, 3094.2.

Acknowledgements

For financial support of this research, we thank the National Natural Science Foundation of China (21225209, 91027043, 51203164), 973 Program (Grant 2011CB932301 and 2013CB933500), NSFC-DFG Joint Project TRR61, and the Chinese Academy of Sciences.

Notes and references

1 (*a*) C. Li, M. Liu, N. G. Pschirer, M. Baumgarten and K. Müllen, *Chem. Rev.*, 2010, **110**, 6817; (*b*) X. Zhan, A. Facchetti, S. Barlow, T. J. Marks, M. A. Ratner, M. R. Wasielewski and S. R. Marder, *Adv. Mater.*, 2011, **23**, 268; (*c*) T. Weil, T. Vosch, J. Hofkens, K. Peneva and K. Müllen, *Angew. Chem., Int. Ed.*, 2010, **49**, 9068.

2 (*a*) B. J. Jung, N. J. Tremblay, M. Yeh and H. E. Katz, *Chem. Mater.*, 2011, **23**, 568; (*b*) H. E. Katz, A. J. Lovinger, J. Johnson, C. Kloc, T. Siegrist, W. Li, Y.-Y. Lin and A. Dodabalapur, *Nature*, 2000, **404**, 478; (*c*) H. Yan, Z. Chen, Y. Zheng, C. Newman, J. R. Quinn, F. Dötz, M. Kastler and A. Facchetti, *Nature*, 2009, **457**, 679; (*d*) D. Shukla, S. F. Nelson, D. C. Freeman, M. Rajeswaran, W. G. Ahearn, D. M. Meyer and J. T. Carey, *Chem. Mater.*, 2008, **20**, 7486; (*e*) X. Guo, F. S. Kim, M. J. Seger, S. A. Jenekhe and M. D. Watson, *Chem. Mater.*, 2012, **24**, 1434; (*f*) S. Bhosale, A. L. Sisson, P. Talukdar, A. Fürstenberg, N. Banerji, E. Vauthey, G. Bollot, J. Mareda, C. Röger, F. Würthner, N. Sakai and S. Matile, *Science*, 2006, **313**, 84.

3 (*a*) F. Würthner and M. Stolte, *Chem. Commun.*, 2011, **47**, 5109; (*b*) X. Lu, Z. Guo, C. Sun, H. Tian and W. Zhu, *J. Phys. Chem. B*, 2011, **115**, 10871; (*c*) A. S. Molinari, H. Alves, Z. Chen, A. Facchetti and A. F. Morpurgo, *J. Am. Chem. Soc.*, 2009, **131**, 2462; (*d*) M. Gsänger, J. H. Oh, M. Könemann, H. W. Höffken, A.-M. Krause, Z. Bao and F. Würthner, *Angew. Chem., Int. Ed.*, 2010, **49**, 740; (*e*) E. M. Giacobbe, Q. Mi, M. T. Colvin, B. Cohen, C. Ramanan, A. M. Scott, S. Yeganeh, T. J. Marks, M. A. Ratner and M. R. Wasielewski, *J. Am. Chem. Soc.*, 2009, **131**, 3700; (*f*) L. Schmidt-Mende, A. Fechtenkötter, K. Müllen, E. Moons, R. H. Friend and J. D. MacKenzie, *Science*, 2001, **293**, 1119; (*g*) C. Li and H. Wonneberger, *Adv. Mater.*, 2012, **24**, 613; (*h*) W. Tan, X. Li, J. Zhang and H. Tian, *Dyes Pigm.*, 2011, **89**, 260.

4 (*a*) L. Tan, Y. Guo, Y. Yang, G. Zhang, D. Zhang, G. Yu, W. Xu and Y. Liu, *Chem. Sci.*, 2012, **3**, 2530; (*b*) X. Gao, C. Di, Y. Hu, X. Yang, H. Fan, F. Zhang, Y. Liu, H. Li and D. Zhu, *J. Am. Chem. Soc.*, 2010, **132**, 3697; (*c*) S. Katsuta, K. Tanaka, Y. Maruya, S. Mori, S. Masuo, T. Okujima, H. Uno, K. Nakayama and H. Yamada, *Chem. Commun.*, 2011, **47**, 10112; (*d*) Z. Yuan, Y. Xiao and X. Qian, *Chem. Commun.*, 2010, **46**, 2772; (*e*) Y. Li, W. Xu, S. Di Motta, F. Negri, D. Zhu and Z. Wang, *Chem. Commun.*, 2012, **48**, 8204; (*f*) C. L. Eversloh, C. Li and K. Müllen, *Org. Lett.*, 2011, **13**, 4148; (*g*) Y. Li, L. Xu, T. Liu, Y. Yu, H. Liu, Y. Li and D. Zhu, *Org. Lett.*, 2011, **13**, 5692; (*h*) Y. Avlasevich, S. Müller, P. Erk and K. Müllen, *Chem.–Eur. J.*, 2007, **13**, 6555; (*i*) Z. Zhang, T. Lei, Q. Yan, J. Pei and D. Zhao, *Chem. Commun.*, 2013, **49**, 2882.

5 (*a*) W. Yue, J. Gao, Y. Li, W. Jiang, S. Di Motta, F. Negri and Z. Wang, *J. Am. Chem. Soc.*, 2011, **133**, 18054; (*b*) J. Gao, Y. Li and Z. Wang, *Org. Lett.*, 2013, **15**, 1366; (*c*) C. Li, C. Xiao, Y. Li and Z. Wang, *Org. Lett.*, 2013, **15**, 682; (*d*) Y. Li, C. Wang, C. Li, S. Di Motta, F. Negri and Z. Wang, *Org. Lett.*, 2012, **14**, 5278; (*e*) W. Jiang, Y. Li, W. Yue, Y. Zhen, J. Qu and Z. Wang, *Org. Lett.*, 2010, **12**, 228; (*f*) Y. Shi, H. Qian, Y. Li, W. Yue and Z. Wang, *Org. Lett.*, 2008, **10**, 2337; (*g*) H. Qian, C. Liu, Z. Wang and D. Zhu, *Chem. Commun.*, 2006, 4587.

6 (*a*) H. Qian, Z. Wang, W. Yue and D. Zhu, *J. Am. Chem. Soc.*, 2007, **129**, 10664; (*b*) H. Qian, F. Negri, C. Wang and Z. Wang, *J. Am. Chem. Soc.*, 2008, **130**, 17970; (*c*) Y. Zhen, C. Wang and Z. Wang, *Chem. Commun.*, 2010, **46**, 1926.

7 (*a*) A. Lv, S. R. Puniredd, J. Zhang, Z. Li, H. Zhu, W. Jiang, H. Dong, Y. He, L. Jiang, Y. Li, W. Pisula, Q. Meng, W. Hu and Z. Wang, *Adv. Mater.*, 2012, **24**, 2626; (*b*) J. Zhang, L. Tan, W. Jiang, W. Hu and Z. Wang, *J. Mater. Chem. C*, 2013, **1**, 3200.

8 W. Yue, A. Lv, J. Gao, W. Jiang, L. Hao, C. Li, Y. Li, L. E. Polander, S. Barlow, W. Hu, S. Di Motta, F. Negri, S. R. Marder and Z. Wang, *J. Am. Chem. Soc.*, 2012, **134**, 5770.

9 L. E. Polander, A. S. Romanov, S. Barlow, D. K. Hwang, B. Kippelen, T. V. Timofeeva and S. R. Marder, *Org. Lett.*, 2012, **14**, 918.

10 (*a*) F. Zhang, Y. Hu, T. Schuettfort, C. Di, X. Gao, C. R. McNeill, L. Thomsen, S. C. B. Mannsfeld, W. Yuan, H. Sirringhaus and D. Zhu, *J. Am. Chem. Soc.*, 2013, **135**, 2338; (*b*) J. Mei, D. H. Kim, A. L. Ayzner, M. F. Toney and

Z. Bao, *J. Am. Chem. Soc.*, 2011, **133**, 20130; (*c*) T. Lei, J. Dou and J. Pei, *Adv. Mater.*, 2012, **24**, 6457; (*d*) H. Chen, Y. Guo, G. Yu, Y. Zhao, J. Zhang, D. Gao, H. Liu and Y. Liu, *Adv. Mater.*, 2012, **24**, 4618.

11 W. Jiang, C. Xiao, L. Hao, Z. Wang, H. Ceymann, C. Lambert, S. Di Motta and F. Negri, *Chem.–Eur. J.*, 2012, **18**, 6764.

12 Y. Li, J. Gao, S. D. Motta, F. Negri and Z. Wang, *J. Am. Chem. Soc.*, 2010, **132**, 4208.

13 C. Huang, S. Barlow and S. R. Marder, *J. Org. Chem.*, 2011, **76**, 2386.

14 Q. Tang, H. Li, M. He, W. Hu, C. Liu, K. Chen, C. Wang, Y. Liu and D. Zhu, *Adv. Mater.*, 2006, **18**, 65.